Influence of solvent on poly(2-(dimethylamino)ethyl methacrylate) dynamics in polymer-concentrated mixtures: a combined neutron scattering, dielectric spectroscopy and calorimetric study

G. Goracci,[*,†] A. Arbe,[†] A. Alegría,[†,‡] V. García Sakai,[¶] S. Rudić,[¶] G.J. Schneider,[§] W. Lohstroh,[‖] F. Juranyi,[⊥] and J. Colmenero[†,‡,#]

Centro de Física de Materiales (CFM) (CSIC–UPV/EHU) – Materials Physics Center (MPC), Paseo Manuel de Lardizabal 5, 20018 San Sebastián, Spain, Departamento de Física de Materiales (UPV/EHU), Apartado 1072, 20080 San Sebastián, Spain, ISIS Facility, Rutherford Appleton Laboratory, Harwell Science & Innovation Campus, Chilton, Didcot, OX11 0QX, United Kingdom, Jülich Centre for Neutron Science JCNS, Forschungszentrum Jülich GmbH, Outstation at MLZ, Lichtenbergstraße 1, 85747 Garching, Germany, Heinz Maier-Leibnitz Zentrum, Technische Universität München, Lichtenbergstraße 1, D-85748 Garching, Germany , Laboratory for Neutron Scattering, Paul Scherrer Institut, CH-5232 Villigen, Switzerland, and Donostia International Physics Center, Paseo Manuel de Lardizabal 4, 20018 San Sebastián, Spain

E-mail: sckgorag@ehu.es

Abstract

We have investigated the dynamical processes –α-relaxation, local motions of the side-groups and methyl group rotations– in poly(2-(dimethylamino)ethyl methacrylate) (PDMAEMA) in the dry state and in mixtures (at 70wt% polymer concentration) with tetrahydrofuran (THF) and water, to address the question how these polymer motions are affected by plasticizers interacting in different ways with the polymer. Differential scanning calorimetry, dielectric spectroscopy and neutron scattering techniques on labelled samples (with deuterated solvents to isolate the signal of the polymer component) have been combined. The α-relaxation is drastically affected, with similar shifts of the glass-transition temperature for both solvents. Effects of compositional heterogeneities and reduction of the fragility are also observed. On the contrary, methyl-group dynamics are unaffected by the presence of solvent. Regarding side-group local motions (β-relaxation), two kinds of components –a slow and a fast one– could be identified in the dry state. Based on the spatial information provided by neutron scattering, a model for the geometry of the motions involved in the fast component has been proposed. Adding solvent, this process would remain essentially unaltered, but the population involved in the slower one would be reduced. With THF as solvent this reduction would be complete, but with water it would be only partial. This could be attributed to rather heterogeneous distribution of water molecules in the polymer likely associated to the presence of water clusters. Such a scenario would also explain the much more pronounced broadening of the glass-transition region observed for the polymer in the aqueous mixture with respect to that induced by THF.

*To whom correspondence should be addressed
†CFM(CSIC–UPV/EHU)/MPC
‡UPV/EHU
¶ISIS
§JCNS
‖MLZ
⊥PSI
#DIPC

I. Introduction

Synthetic polymers are important in fields as food packaging, water treatment and implantable medical devices.[1,2] For example, poly(2-(dimethylamino)ethyl methacrylate) (PDMAEMA) is a polymer commonly investigated for the development of materials with antibacterial properties.[3] PDMAEMA is rich in tertiary amino groups which can be converted to positively charged quaternary ammonium groups with bactericidal properties. Moreover it has been investigated to build gene deliveries in the gene therapy field.[4] So far, viral vectors are the most used gene carriers. However, due to safety issues associated with them, i.e. immune responses or gene mutations, it has been necessary to develop non-viral gene carrier. Among them, polycationic polymers, as PDMAEMA, are now widely used in gene therapy for their chemical properties[5].

In the practical use, many polymeric materials contain plasticizers (low molecular weight additives) to tailor the physical properties to technical needs. Many of these properties are connected to the molecular mobility in the system. Dynamic processes in polymers occur over a wide range of length and time scales.[6] Above the glass transition temperature T_g the structural or α-relaxation takes place. This process is characterized by a strong temperature dependence of its characteristic time: cooling the system, the dynamics slows down and it "freezes" approaching T_g. Below this temperature, only local processes are detectable, as methyl group rotations and secondary relaxations like the so-called β-process. The main effect of the presence of plasticizers on the dynamics is a reduction of the glass transition temperature (plasticization effect), but they might also influence the other dynamical processes in the system. The aim of this work is to determine how these molecules affect the polymer dynamics at different levels and to investigate the role of the solvent/polymer interaction. In biological systems, where water is the ubiquitous solvent, the formation of hydrogen bonds has to play a crucial role in this game. Therefore, a comparative study considering water and other solvent where this kind of interactions are absent could be important to disentangle the origins of the observed effects.

With these ideas in mind, the system chosen for this investigation was PDMAEMA in concentrated mixtures with either water or tetrahydrofuran (THF). In both cases the polymer concentration was 70 wt%. The dry polymer was also investigated as reference. Both, THF and water are good solvents for this polymer. THF does not interact via H-bonds with the polymer contrarily to water, where H-bonds are the main source of solvent-polymer (and solvent-solvent) interactions. This property allows us addressing the question of the influence of the nature of these interactions on the effect on the dynamics of the polymer component. Combining dielectric spectroscopy (DS) and neutron scattering (NS) techniques (both, quasielastic and inelastic), we have covered a broad frequency and temperature range. Differential scanning calorimetry (DSC) has also been employed. For the scattering experiments the plasticizers have been deuterated to make them almost transparent for neutrons. Three kinds of processes –besides vibrations– taking place in the polymer have been identified and investigated: the α-relaxation, localized motions involving the lateral group and methyl group rotations. The latter have been specifically studied by inelastic neutron scattering techniques through the librational peaks present in the vibrational density of states at low temperature. This investigation has provided the full characterization of the rotational dynamics of the different methyl groups in the polymer. Such information is not only valuable *per se*, but also because it allows fixing the contribution of methyl-group rotations in the analysis of the quasielastic spectra, facilitating thereby their interpretation. The application of a consistent unified methodology has allowed combining the information provided by the different techniques employed in a synergetic way.

II. Experimental Section

A. Samples

PDMAEMA (see monomeric chemical formula in Fig. 1) was purchased from Polymer Source. The average molecular weight of the polymer is $M_w = 57000$ g/mol, with polydispersity

M_w/M_n= 3.0. Polymer as received was annealed for 7 h at T = 373 K under vacuum to evaporate possible trapped solvent, while the mixtures containing 30 wt% of solvent were prepared by mixing the dry polymer with the appropriate amounts of THF, dTHF, H_2O or D_2O (Sigma Aldrich) during a few days. DS and DSC experiments were performed on samples with protonated solvents, while those with deuterated solvents were used to isolate the polymer component in the NS experiments.

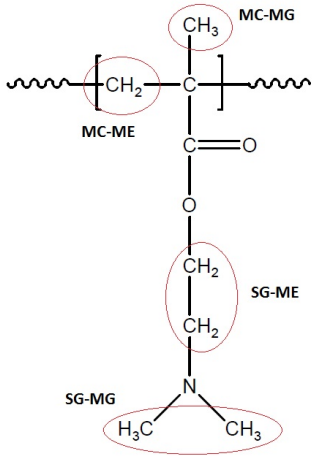

Figure 1: Chemical formula of PDMAEMA

B. Quasielastic Neutron Scattering (QENS)

In quasielastic neutron scattering (QENS) experiments, the distribution of energy changes ($\hbar\omega$) of the neutrons scattered into a solid angle is analyzed (see, as general references,[7–9]). The intensity measured contains contributions from all nuclei from the sample, weighted by the corresponding scattering cross sections. Since the incoherent cross section of hydrogen $\sigma_{H,inc}$ is much higher than any other cross section of the nuclei composing our samples, the scattered intensity is largely dominated by the incoherent component of the hydrogens, revealing thus their incoherent scattering function, $S_{inc}(Q,\omega)$ (Q: modulus of the scattering vector) determined by the *self-dynamics*.

Four QENS spectrometers were used: the direct-geometry time-of-flight instruments FOCUS (PSI, Villigen, Switzerland) and TOFTOF (MLZ, Garching, Germany), the inverted-

geometry time-of-flight spectrometer IRIS (ISIS, Didcot, UK) and the backscattering spectrometer SPHERES (JCNS, Garching, Germany). Each sample was investigated using a combination of spectrometers and/or incident wavelengths (see Table 1), in order to cover a wide dynamic window. The time windows accessed were approximately from 10^{-13} to 10^{-9} s for the polymer in dTHF and deuterated water solutions and from 10^{-12} to 10^{-10} s for the dry sample.

Table 1: Experimental configurations used for QENS measurements.

Sample	Instrument	incident wavelength (λ) (Å)(* analysing energy)	energy resolution (FWHM) (μeV)
PDMAEMA/*THF*	FOCUS	6.0	~ 45
	IRIS	6.65 *	17.5
	SPHERES	6.27 *	0.62
PDMAEMA/D_2O	TOFTOF	6.0	~ 48
	TOFTOF	7.0	~ 25
	SPHERES	6.27 *	0.62
PDMAEMA	TOFTOF	6.0	~ 55
	TOFTOF	8.0	~ 25

For all experiments, flat aluminium sample holders were used. For the samples in solution, the cells were sealed using indium wire to avoid solvent loss. The thicknesses of the sample holders were chosen in order to obtain a transmission close to 90% to neglect possible multiple scattering contributions. Vanadium in flat aluminum cell was measured at room temperature to correct the detector efficiency. All data were corrected for the sample holder contribution by subtracting the intensity scattered by an empty cell. The resolution function was determined measuring the samples at 10 K. Dry PDMAEMA and PDMAEMA/dTHF samples were investigated at T = 250 K, 270 K, 290 K, while the PDMAEMA/D_2O system was studied at T= 250 K. For the ulterior analysis of the QENS results, data were transformed into time domain, following a procedure which allows deconvolution of data from the instrumental resolution, thereby facilitating the combination of results from different spectrometers. Experimental intermediate scattering functions $S^{exp}(Q,t)$ were obtained by

Fourier transforming to time domain the QENS data measured at a given temperature and Q-value on each spectrometer. These functions were deconvoluted from the resolution function dividing them by the corresponding $S^{exp}(Q,t)$ obtained from the spectrum measured at 10 K.

C. Inelastic Neutron Scattering (INS)

Information on methyl-group dynamics is provided by the inelastic librational peaks contained in the vibrational density of states (VDOS) at low temperature. This function was measured by using TOSCA (ISIS, Didcot, UK). TOSCA is an indirect geometry spectrometer spanning an energy-transfer range up to 4000 cm^{-1} (500 meV) in neutron energy loss. The dry sample was loaded in an aluminium foil sachet closed in a flat aluminium sample holder sealed by indium wire, while for the mixtures indium wire-sealed liquid cells were used. All samples were investigated at T = 10 K.

D. Dielectric Spectroscopy and Calorimetry

Broadband dielectric spectrometer Novocontrol Alpha-S and high frequency dielectric spectrometer Agilent E4991A RF-Impedance Analyzer were used to measure the complex dielectric function $\epsilon^*(\omega) = \epsilon^{'}(\omega) - i\epsilon^{''}(\omega)$, covering a frequency range of 10^{-2}-10^9 Hz. The samples were prepared forming a parallel-plate capacitor between parallel gold-plated electrodes with a diameter of 20 and 10 mm for low and high frequency measurements respectively. Measurements were carried out under isothermal conditions every 5 K with a temperature stability better than 0.1 K. The maximum temperature for the dry polymer (370 K) was chosen to avoid degradation, while for the plasticized samples we performed measurements up to 300 K to avoid a significant solvent evaporation. Differential scanning calorimeter (DSC) TA Instrument Q2000 was used to determine the glass transition temperature T_g of the samples (sample weights about 10 mg). Hermetic aluminium pans were used for all the samples. Modulated DSC measurements were performed on PDMAEMA, PDMAEMA/THF

and PDMAEMA/H_2O with average heating rate of 3 K/min and amplitude of modulation ± 0.5 K with a period of $t_p = 60$ s.

III. Results and Data Analysis

A. Dielectric Spectroscopy and Calorimetry

Dielectric spectroscopy measurements on dry PDMAEMA reveal two broad temperature-dependent processes (Fig. 2). The main peak, relevant at higher temperatures, is related to the segmental (α) relaxation while that at low temperature can be attributed to a secondary relaxation. Adding THF we observe a strong shift toward lower temperature of the main peak. Actually, this contribution becomes a kind of shoulder superimposed to the strong conductivity which dominates at high temperatures. The shift of the α-relaxation is associated to the change of T_g, as confirmed by DSC experiments (inflection point at T_g^{DSC}(PDMAEMA) = 299 K, $T_g^{DSC}(PDMAEMA/THF) = 227$ K). The secondary relaxation peak in PDMAEMA/THF appears slightly shifted (~ 20 K) toward higher temperature with respect to that in bulk. We note that these data result from the combined contributions of the two components in the system (polymer/THF). In PDMAEMA/H_2O only an intense peak in the low temperature region is present. This peak is related to the dynamics of water molecules and seemingly covers the polymer secondary relaxation due to the high signal given by the strong water dipole moment. At high temperature it is not possible to distinguish the segmental relaxation in this sample due to the huge conductivity contribution.

In the high temperature region above T_g, polymer motions are dominated by the α-relaxation. In such regime, the dielectric permittivity of polymers can usually be fitted with the sum of the contributions from the α-relaxation (described by a Havriliak-Negami function) and the conductivity (see, as general reference for dielectric data analysis, Ref. [10]):

$$\epsilon^*(\omega) = \epsilon^{'}(\omega) - i\epsilon^{''}(\omega) \; = \; \epsilon_\infty + \frac{\Delta\epsilon}{[1 + (i\omega\tau_{HN})^\alpha]^\beta} - i\frac{\sigma_0}{\epsilon_0\omega} \tag{1}$$

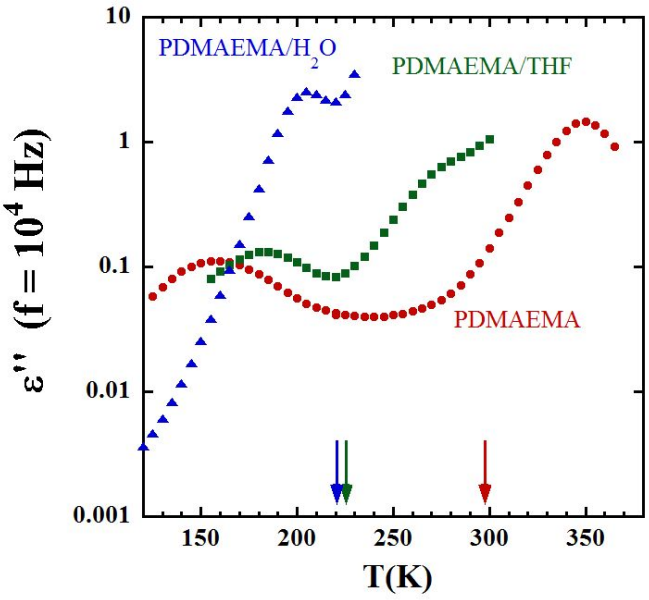

Figure 2: Isochronal curves of dielectric loss obtained for $f = 10^4\ Hz$. Blue triangles: PDMAEMA/H_2O; green squares: PDMAEMA/THF; red circles: PDMAEMA. Arrows show the locations of T_g determined from DSC (inflection point), T_g^{DSC}

.

Here, ϵ_∞ is the high-frequency limit permittivity, $\Delta\epsilon$ is the dielectric strength, τ_{HN} is the characteristic relaxation time, α and β are the shape parameters of the α-process, σ_0 is the DC conductivity and ϵ_0 is the vacuum permittivity. Usually the data analysis is performed on the imaginary part of the permittivity $\epsilon^{''}(\omega)$, where the relaxation process leads to a peak. This was the procedure followed in the case of the dry polymer (see Fig. S1 in the Supporting Information as a representative example). However, adding THF, it is not possible to clearly resolve the high temperature process (α-relaxation of the polymer) from the large conductivity contributions to $\epsilon^{''}(\omega)$ (see, e.g, Fig. 3(a)). Therefore, the data analysis was carried out on the real part of $\epsilon^*(\omega)$, $\epsilon^{'}(\omega)$, where conductivity does not contribute. I n partic ular, we considered the derivative of $\epsilon^{'}(\omega)$ with respect to $\log(\omega)$, since this function displays a maximum at similar frequency as the $\epsilon^{''}(\omega)$ relaxational counterpart.[10,11] The data of the PDMAEMA/THF sample were fitted by:

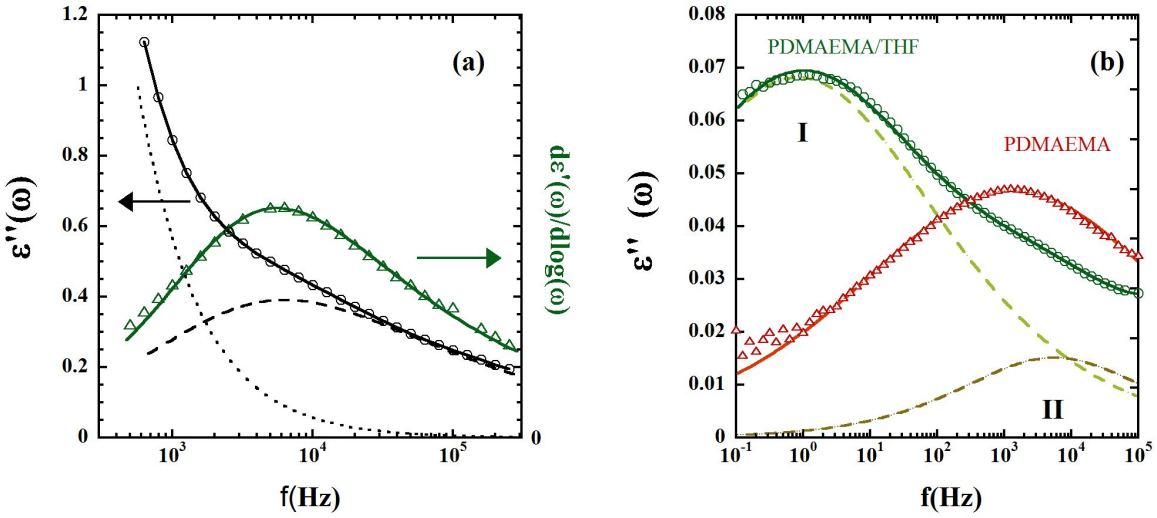

Figure 3: **a**)DS results at high temperature (T=270 K) showing the α-relaxation contribution of PDMAEMA/THF mixture. Circles show the experimental $\epsilon''(\omega)$ described by the imaginary part of eq. 1 (continuous line). Dashed line represents HN function and dotted line the conductivity contribution. Triangles show the derivative $\partial\epsilon'(\omega)/\partial log(\omega)$ fitted by eq. 2 (continuous line). **b**) Results on PDMAEMA/THF (circles) and the dry polymer (triangles) at 130 K, in the glassy state. For comparative purposes, bulk polymer data have been multiplied by 0.7 in order to take into account the amount of polymer in the mixture. The dashed lines show the two Cole-Cole components used to describe PDMAEMA/THF data.

$$\frac{\partial\epsilon'(\omega)}{\partial \log\omega} \propto \Re\left[\frac{(i\omega\tau_{HN})^{\alpha}}{[1+(i\omega\tau_{HN})^{\alpha}]^{\beta+1}}\right]. \tag{2}$$

The quality of the fit is shown in Fig. 3(a) and in Fig. S2 of the Supporting Information for several temperatures investigated. For both systems, dry PDMAEMA and PDMAEMA/THF, from the obtained values of the Havriliak-Negami parameters –τ_{HN}, α and β– the characteristic time τ_{max} was calculated using the relationship:[10]

$$\tau_{max} = \tau_{HN}\left[\frac{\sin(\frac{\alpha\beta\pi}{2+2\beta})}{\sin(\frac{\alpha\pi}{2+2\beta})}\right]^{1/\alpha} \tag{3}$$

This time is defined as the inverse of the frequency ω_{max} at the $\epsilon''(\omega)$-peak, $\tau_{max} = 1/\omega_{max}$.

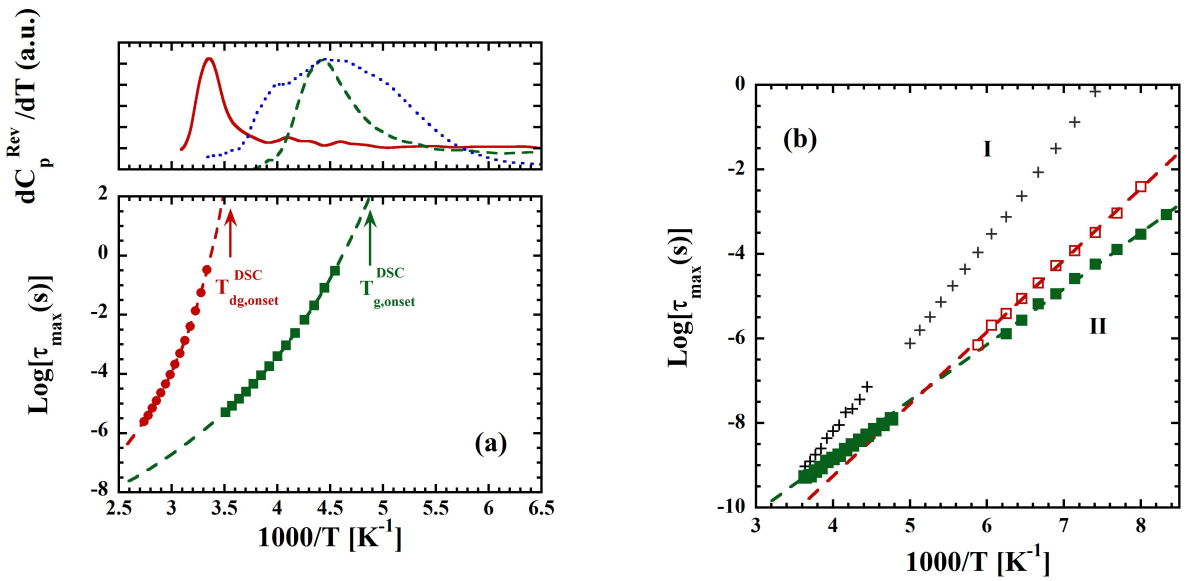

Figure 4: **a**) Top: Temperature derivative of the reversible specific heat of PDMAEMA (red solid line), PDMAEMA/THF (green dashed line) and PDMAEMA/H_2O (blue dotted line). Arrows mark the position of the onset temperature for the DSC glass transition. Bottom: Inverse temperature dependence of the characteristic times of the α-relaxation obtained from DS. Red circles represent data from PDMAEMA in the dry state, while green squares in the mixture with THF. Dashed lines are fits with the VFT expression (Eq. (4)). **b**) Relaxations attributable to the polymer component in the dry state (empty red squares) and in PDMAEMA/dTHF (filled green square, 'process II'). Crosses correspond to 'process I', which is attributed to THF contributions.

Due to the high conductivity produced by water molecules, it is not possible to observe the structural relaxation of PDMAEMA in aqueous solution even using the representation $\partial\epsilon'(\omega)/\partial\log(\omega)$. Figure 4(a) shows the inverse-temperature dependence of the relaxation times obtained for the α-process of dry PDMAEMA and PDMAEMA/THF samples. The curvature clearly shows the non-Arrhenius character expected for the dynamics in the supercooled liquid state. The curves were fitted with the usually invoked Vogel-Fulcher-Tammann (VFT) equation:[12–14]

$$\tau = \tau_0 \exp\left(\frac{B}{T - T_0}\right). \tag{4}$$

VFT parameters are shown in Table 2.

The fragility index m, describing how fast dynamics change approaching the glass tran-

sition temperature, is mathematically defined as:[15]

$$m = \left.\frac{\partial \log\tau}{\partial(T_g/T)}\right|_{T=T_g} \tag{5}$$

We calculated this index starting from VFT results and defining $T_g = T_g^{DS}$ as the temperature at which the relaxation time reaches a value of 100 s. The T_g^{DS} values of PDMAEMA in the dry state and in the mixture with THF are shown in Table 2, in comparison with the values deduced from DSC measurements. This table also includes the such obtained values of m.

The spectral shape of the α-process differs, as usually found, from that of a single Debye process. The width of this relaxation is represented as function of the characteristic time in Fig. 5(a) for both systems.

Table 2: Vogel-Fulcher-Tammann parameters of the characteristic time of the α-relaxation and fragility index of PDMAEMA in the dry state and with THF. T_g values determined from DS and DSC are also given for the three systems. For DSC, values correspond to the inflection point of the $C_p(T)$ (T_g^{DSC}) and to its onset ($T_{g,onset}^{DSC}$)in the heating ramp.

	PDMAEMA	PDMAEMA/THF	PDMAEMA/H_2O
$\log(\tau_0(s))$	-11.7 ± 0.1	-11.4 ± 0.1	-
B(K)	1666 ± 6	1881 ± 6	-
T_o(K)	231.1 ± 0.3	142.0 ± 0.3	-
T_g^{DS}(K)	287 ± 1	204 ± 1	-
T_g^{DSC}(K)	299 ± 1	227 ± 1	220 ± 3
m	148	95	-
$T_{g,onset}^{DSC}$(K)	285 ± 1	205 ± 1	176 ± 1

At lower temperatures –below T_g– only local motions leading to secondary relaxations are expected to take place. In Fig. 3(b) spectra of dry PDMAEMA and PDMAEMA/THF are shown at $T = 130$ K. The dry sample shows a broad and nearly symmetric peak –the polymer β-relaxation– suggesting a distribution of mobilities. In order to describe this contribution, a Cole-Cole function –i.e, a Havriliak-Negami function with $\beta \equiv 1$– was used:[10]

$$\epsilon^*_{CC}(\omega) = \epsilon_\infty + \frac{\Delta\epsilon}{[1 + (i\omega\tau_{CC})^{\alpha_{cc}}]} \tag{6}$$

with τ_{CC} ($\equiv \tau_{max}$) the Cole-Cole characteristic relaxation time and α_{CC} the shape parameter. In PDMAEMA/THF two dynamic processes can be distinguished in this temperature range; therefore, a combination of two Cole-Cole functions was used in the fitting procedure (see the two contributions as dashed lines in Fig. 3(b)). Fits over the whole temperature range investigated are shown in Figs. S3 and S4 of the Supporting Information for the two samples. The characteristic times obtained from such description of the dielectric results of PDMAEMA in the dry state and in the mixture are shown in Fig. 4(b).

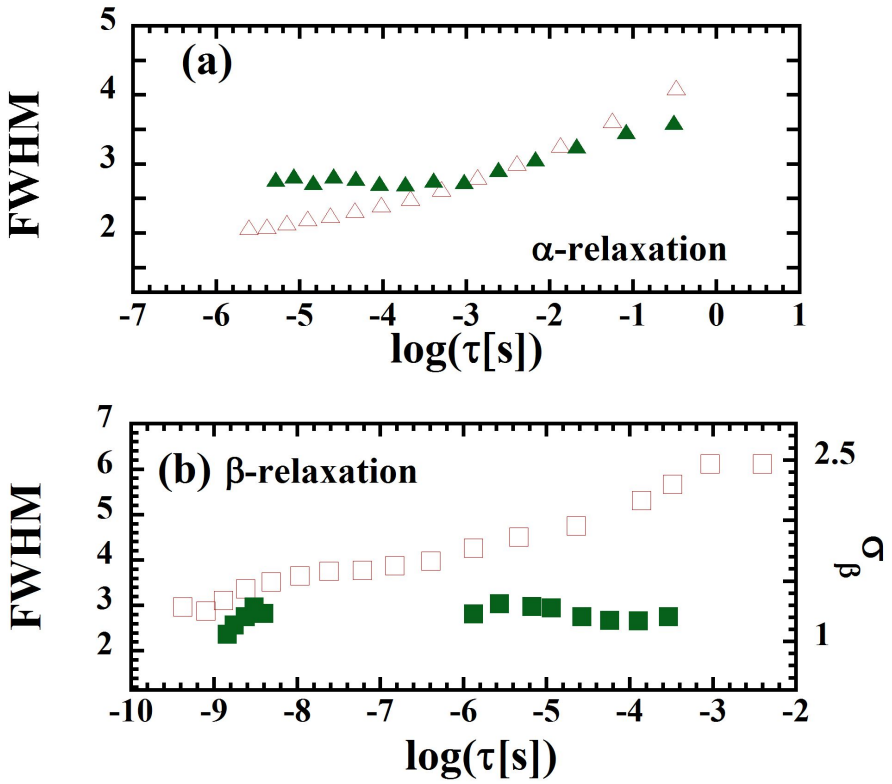

Figure 5: Full width at half maximum[16] of loss peak corresponding to the α-relaxation (a) and β-relaxation (b) of the polymer as function of the characteristic time. Empty symbols refer to dry PDMAEMA, while filled symbols to PDMAEMA/THF. In (b), the scale on the right shows the equivalent width of the corresponding Gaussian distribution of relaxation times σ_β.

At this point, we discuss on the origin of the two different secondary relaxation processes observed in the glassy state of the PDMAEMA/THF mixture (we will call them 'process I' –that occur at lower frequency– and 'process II' –that is contributing at higher frequency–). Based on the strong intensity of process I, it has to be attributed to a relaxation involving THF molecules. Its interpretation is presented in a complementary work on the THF component including QENS experiments on the inversely labelled system.[17] Here we note that a similar process has been reported for mixtures of THF with trisyrene[18] and also for other binary solvent/polymer mixtures like that investigated in Refs.[19,20] To interpret the origin of 'process II', in Fig. 3(b) we have included the β-relaxation results obtained for the dry polymer at the same temperature, properly weighted in order to represent the expectation fo r the β-contribution of the polymer –if it were unaffected by the presence of the solvent– in the permittivity loss measured on the mixture with THF. The characteristic time of this contribution is clearly faster than that of the 'process I' of the PDMAEMA/THF system, but it is rather close to that corresponding to the 'process II'. We thus may identify the 'process II' in PDMAEMA/THF as the β-relaxation of the polymer component. We note, however, that this relaxation is affected by the presence of THF molecules.

As expected for thermally activated processes, the relaxation times characteristic for the sub-T_g relaxations follow an Arrhenius temperature dependence:[10]

$$\tau = \tau_o \exp\left(\frac{E_a}{k_B T}\right) \tag{7}$$

with the parameters shown in Table 3.

Table 3: Arrhenius parameters of the characteristic time of the β-relaxation in dry PDMAEMA and in THF mixture

		PDMAEMA/THF	
	dry PDMAEMA	PDMAEMA	THF
$\log[\tau_o(s)]$	-16.1 ± 0.1	-14.1 ± 0.2	-17.5 ± 0.2
E_a(kJ/mol)	32.5 ± 0.5	28.5 ± 0.5	44.3 ± 0.9

Symmetric broadening of spectra can be attributed to the presence of distributions of

relaxation times in the glassy state due to the disorder. We may consider the logarithmic relaxation times distributed according to a Gaussian function:

$$h[log(\tau)] \;=\; \frac{1}{\sqrt{2\pi\sigma^2}}\exp\left(-\frac{\left[\log(\tau)-\overline{\log(\tau)}\right]^2}{2\sigma^2}\right) \tag{8}$$

Here, $\overline{log(\tau)}$ is the average logarithm of the characteristic time (position of the maximum of the distribution function), $\overline{log(\tau)} \equiv log(\tau_{CC})$. For the β-process, the width of such distribution (we shall call it σ_β) has been calculated starting from the shape parameter α_{CC} of the Cole-Cole function by the empirical equation[21] :

$$\sigma_\beta \;=\; \frac{6.9\times10^{-4}}{\alpha_{CC}^4} - 3.8163\log(\alpha_{CC}) \tag{9}$$

The so-obtained results are represented in Fig. 5(b) as function of the characteristic time.

B. Neutron Scattering

Due to the high value of the hydrogen incoherent cross section, the function accessed by neutron scattering is mainly dominated by the incoherent scattering function from all the hydrogens in the sample (i. e., belonging to PDMAEMA). This is composed by the superposition of those of the individual hydrogens as: $S(Q,t) = N^{-1}\sum_{\alpha=1}^{N} S^\alpha(Q,t)$ (in the following, we will skip the label 'inc'), where the index α refers to the kind of hydrogen in the PDMAEMA component. So, α can be: main-chain methylene hydrogen (MC-ME) (2 hydrogens out of 15 per monomer unit); main-chain methyl-group hydrogen (MC-MG) (3 out of 15); side-group methylene hydrogen (SG-ME) (4 out of 15) or side-group methyl-group hydrogen (SG-MG) (6 out of 15). Figure 6 shows as an example the experimentally obtained intermediate scattering functions in the PDMAEMA/dTHF sample for some representative Q-values and two different temperatures. As can be seen, by applying the above described deconvolution procedure to data measured on three spectrometers (FOCUS, IRIS

and SPHERES in this case), almost three decades in time are covered. The intermediate scattering functions show more pronounced decays at higher temperatures, with a tendency to reach a plateau in the long-time regime. For a given temperature, the characteristic time for the decay does not show a clear Q-dependence. These features suggest the occurrence of spatially localized motions in the window investigated.

In general, the intermediate scattering function describing a localized motion is given by (see, as a general reference,[7])

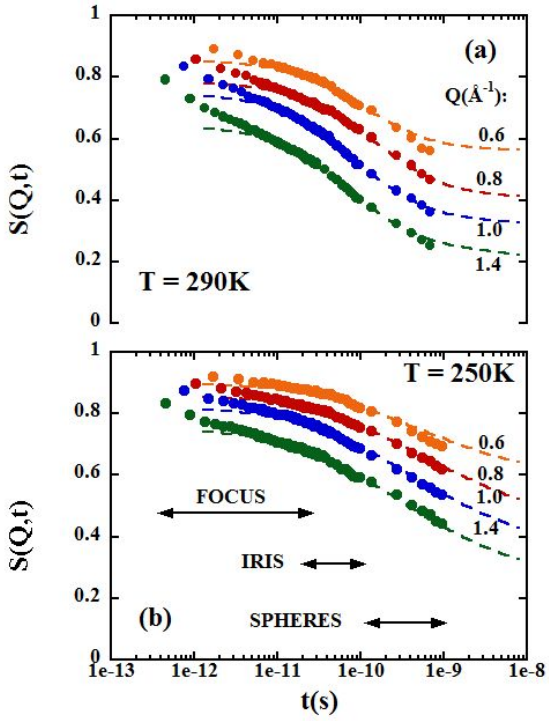

Figure 6: Intermediate scattering function of H-atoms of the polymer component in the PDMAEMA/dTHF sample at T = 290 K (top) and T = 250 K (bottom) and the different Q-values indicated. The dashed lines show the fits with the model described in the text.

$$S_{loc}(Q,t) = EISF + (1 - EISF)\phi(t) \tag{10}$$

where the elastic incoherent structure factor (EISF) contains the information about the geometry of the motion and the function $\phi(t)$ the dynamic information (time dependence). Due to the heterogeneities of the amorphous systems investigated, in the general case we expect $\phi(t)$ to result from a distribution of single exponential functions:

$$\phi(t) \; = \; \int h[log(\tau)]\exp(-t/\tau)\mathrm{d}log(\tau) \tag{11}$$

A pre-factor A multiplying Eq. 10 is usually also needed. This pre-factor parametrizes the fast contributions (fast motions like vibrations leading to the decay of correlations at times shorter than those accessible by the instruments). For the sake of simplicity, we assumed this vibrational parameter to be the same for all hydrogen atoms in PDMAEMA. Now we define the model functions for each kind of hydrogen in our polymer.

(i) *Main-chain hydrogens*:

(i.a) *Main-chain methylene hydrogens.* Given the temperature range investigated, we assumed in a first approximation that segmental motions are too slow for the neutron scattering window. This implies that main-chain methylene hydrogens only vibrate around their equilibrium positions leading to an elastic contribution accounted for by the previously defined parameter A.

(i.b) *Main-chain methyl-group hydrogens.* Superimposed to the vibrations, MC-MG hydrogens may rotate. We will refer to the scattering function of MC-MG hydrogens corresponding to such rotations as $S_{MG}^{MC-MG}(Q,t)$, and will give later the details to build it.

(ii) *Side-group hydrogens.* By dielectric spectroscopy we have detected and characterized a secondary (β) relaxation related to the polymeric component. The reorientational motions of the dipole moment –located in the side-group– giving rise to this relaxation, could then be attributed to dynamical processes involving the side-group atoms in PDMAEMA. We would then expect that the dynamic function describing the time evolution of the localized atomic motions underlying the β-process –we shall call it $\phi_{SG}(t)$– could reflect the distribution of

mobilities observed by dielectric spectroscopy (i. e., Eq. 11 with Eq. 8 and Eq. 9). We thus have assumed for this function $\phi_{SG}(t)$ a distribution of exponentials corresponding to a Gaussian distribution of $\log(\tau_{SG})$. Regarding the EISF characterizing these localized processes, a plausible geometry would be that of a confined motion on a disc of radius R:

$$EISF_{SG} = \frac{1}{6}\left(1 + 2j_0(QR) + 2j_0(QR\sqrt{3}) + j_0(2QR)\right) \tag{12}$$

This kind of geometry was found to work describing the incoherent scattering function of hydrogens in polyethylene[22] (PE). The spatial extent of the motion –parametrized by the radius R– would depend on the particular kind of hydrogens within the side-group (note that all hydrogens in the side-group shall participate in this process).

(ii.a) *Side-group methylene hydrogens.* These atoms are assumed to undergo vibrations and the above-described side-group motions within a disc. We found that a suitable value for R was 3Å, which is rather close to that reported for hydrogen motions in semicrystalline PE[22]. Thus, we fixed the value of this parameter to $R \equiv 3$ Å in the subsequent analysis.

(ii.b) *Side-group methyl-group hydrogens.* In this case, we estimated that the radius of the disc is determined by the distance between the centers of mass of the methyl groups (this distance is 3.3Å). That is, $R \equiv r_{SG-MG} = 1.65$Å. Moreover, we considered the contribution of the methyl group rotations, characterized by the scattering function $S_{MG}^{SG-MG}(Q,t)$. We will deal with this function later. Assuming simultaneous occurrence of both localized motions (side-group localized motions on a disc and rotations around the corresponding methyl carbon), the total intermediate scattering function for SG-MG hydrogens was built as the product of the two functions corresponding to these individual processes.

Summarizing, the model intermediate scattering function used to describe the expected

local contributions to QENS results was:

$$S_{loc}(Q,t) = A\{\frac{2}{15} + \frac{3}{15}S_{MG}^{MC-MG}(Q,t) + \\ + \frac{4}{15}\left[EISF_{SG}^{SG-ME} + (1 - EISF_{SG}^{SG-ME})\phi_{SG}(t))\right] + \\ + \frac{6}{15}\left[EISF_{SG}^{SG-MG} + (1 - EISF_{SG}^{SG-MG})\phi_{SG}(t))\right] S_{MG}^{SG-MG}(Q,t)\} \quad (13)$$

Now we consider in detail the contributions of methyl-group rotations. In the glassy state of polymeric materials the interaction between the methyl group and its environment is often well approximated by an effective mean-field rotational potential (see, as general reference, Ref.[23]). In the simplest approximation this potential is threefold $V(\phi) = V_3\left[1 - cos(3\phi)\right]/2$ and the potential barrier V_3 determines both, the activation energy of the stochastic jumps occurring at high temperature –contributing to the quasielastic window– and the librational energies –in particular, that corresponding to the lowest librational transition E_{01}– which are detectable in the VDOS at low temperature. Therefore, TOSCA experiments were of utmost importance in this work, since they allowed an independent characterization of the methyl group dynamics of PDMAEMA in the three samples investigated. TOSCA results are shown in Fig. 7. We do not find any significant difference, e. g. an energy shift or an extra broadening, between the three sets of data. Thus, at first sight, one can realize that the effect of plasticizers on these peaks, if any, is negligible. The VDOS present a pronounced and relatively broad peak centred at about 33 meV followed by other less intense peaks. The first two peaks are in the energy range where the first librational transition usually manifest[23]. We may assume that they correspond to the two kinds of methyl group in PDMAEMA. Since the area of the first peak was about two times the area of the second one, we related the former to the librations of the methyl groups of the side chain (SG-MG), and the latter to the libration of the methyl group of the main chain (MC-MG). To describe the data we invoked the rotational rate distribution model (RRDM),[23–25] that assumes a Gaussian distribution of potential barriers with $\overline{V_3}$ the average value and σ_{V_3} the standard deviation

of the distribution. The origin of this distribution is the disorder inherent to the glassy materials. In the Supporting Information the complete details of the fitting procedure of TOSCA results and the application of the RRDM can be found. The obtained values for $\overline{V_3}$ and σ_{V_3} are listed in Table 4. Once the distribution of V_3 is known for a given kind of methyl group α, the corresponding intermediate scattering function $S^{\alpha}_{MG}(Q,t)$ can be constructed as it is explained in the Supporting Information.

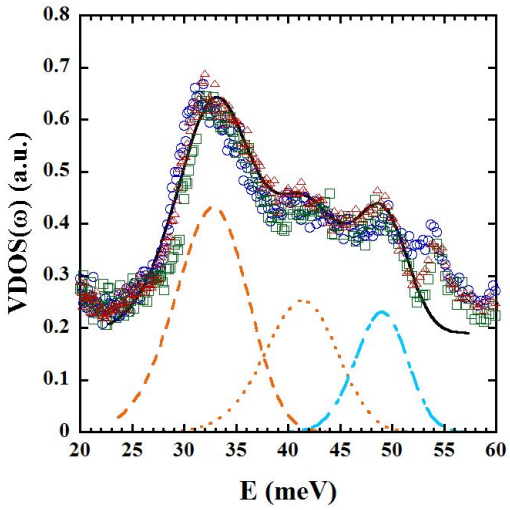

Figure 7: H-weighted vibrational density of states of PDMAEMA in the dry state (red triangles), and in the mixtures with *d*THF (green circles) and with D_2O (blue squares) at T = 10 K. The intensities of the mixtures have been scaled to match that of dry PDMAEMA. Solid line is a fit with the different contributions indicated by the dotted, dashed and dashed-dotted lines. Further details can be found in the Supporting Information.

Table 4: Parameters characterizing the methyl-group dynamics of dry PDMAEMA and PDMAEMA in mixtures with $dTHF$ and with D_2O obtained from TOSCA experiments.

Parameters	SG-MG			MC-MG		
	Dry	THF	D_2O	Dry	THF	D_2O
$\overline{V_3}$(K)	2293	2344	2193	3449	3541	3374
σ_{V_3}(K)	410	390	435	455	435	505

Having completely fixed the contributions from methyl-group rotations [$S^{MC-MG}_{MG}(Q,t)$ and $S^{SG-MG}_{MG}(Q,t)$] from the TOSCA study, the fit of the QENS results with Eq. 13 was

possible. As it has been mentioned above, we also fixed the rest of parameters (radii of the discs R) characterizing the geometry of the motions of the hydrogens of PDMAEMA. Thus, the only free parameters left were A, and σ and $\overline{\log(\tau)}$ in $\phi_{SG}(t)$.

Analysis of PDMAEMA/dTHF QENS data. We started with these results, which are of the best quality (wider dynamic window and T-range and time-scale of localized SG-motions better centered in the QENS window). At 250 K, the width of the distribution of the relaxation times of side-group motions was fixed imposing the σ_β obtained from DS results on the β-process (see Fig. 5(b)). The only free parameters were then the pre-factor A and the average characteristic time for the localized motion of hydrogens underlying the β-relaxation. The so obtained curves match very well the data at times longer than approximately $\sim$ 10 ps, as shown in Fig. 6(b). The values obtained for the average logarithm of the characteristic time for the side-group motion [$\overline{\log(\tau)}$ in Eq. 8] are displayed in Fig. 8 as function of Q. They are practically Q-independent, as it would be expected for a localized motion. The resulting Q-averaged value $< \overline{\log(\tau)} >_Q$ agrees very well with the DS time $\overline{\log(\tau_{DS})}$ (see Fig. 9). Such a nice agreement fails at higher temperatures. Good fits (see e. g. Fig. 6(a)) were obtained with $< \overline{\log(\tau)} >_Q$ values (shown in Fig. 9 as empty circles) nearly indistinguishable from those extrapolated from the DS, but using narrower distributions (e. g. for 290 K, σ_β $\sim$0.48 from QENS vs 1.03 from DS).

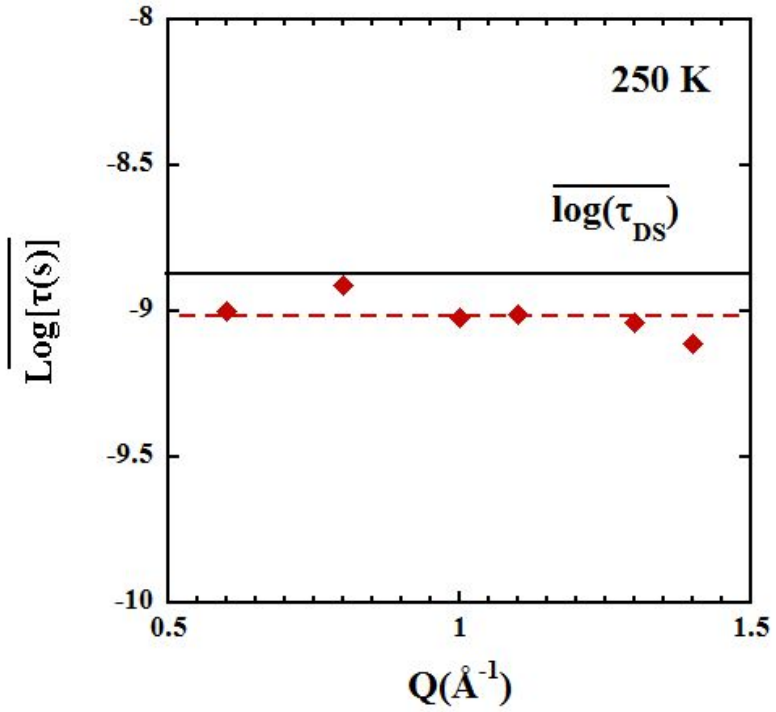

Figure 8: Momentum-transfer dependence of the average characteristic time associated to the local dynamics of side-group hydrogens in PDMAEMA in mixture with THF obtained from QENS at 250 K. Solid line indicates the result from the dielectric study on the β-relaxation at the same temperature. Dotted line shows the Q-averaged value of the QENS result $< \overline{\log(\tau)} >_Q$.

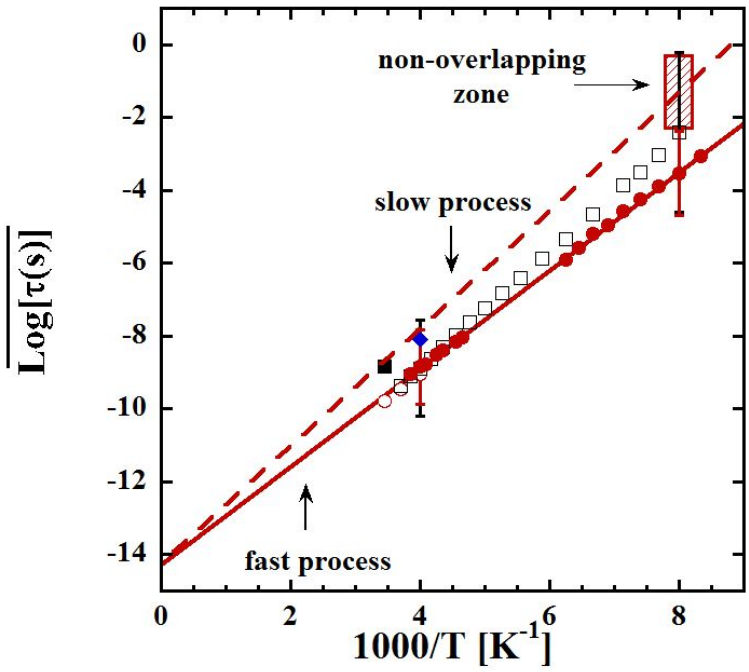

Figure 9: Arrhenius plot of the relaxation times of the polymer component revealed by DS in THF mixture (Process II, red filled circles) and dry PDMAEMA (empty squares). The Q-averaged QENS results are represented as empty circles for PDMAEMA/dTHF, blue diamond for PDMAEMA/D_2O and filled square for dry PDMAEMA. In these fits, Eq. 13 was used (f=1 in Eq. 16 has been assumed (see the text)). Solid line is an Arrhenius fit of the DS data of PDMAEMA in the mixture with THF, which is assumed to represent the fast component of the β-relaxation in the dry system. Dashed line is the deduced slow component of this process (see the text). Bars represent the width of the distribution function deduced from the values of the FWHM shown in Fig. 5(b).

We note that 270 and 290 K are relatively high with respect to T_g in the mixture. Therefore, the observed narrowing could be an apparent effect due to the additional dynamics –α-relaxation– superimposed to the localized motions at such high temperatures. We have thus alternatively fitted the QENS data at 290 K by assuming the occurrence of statistically independent α- and β-processes.[10] The α-process was characterized by a stretched exponential intermediate scattering function:

$$S_\alpha(Q,t) \,=\, \exp[-(t/\tau_w)^\beta] \tag{14}$$

with the β-parameter fixed as determined from the DS analysis ($\beta \,=\, 0.38$ for T=290 K). The model scattering function was thus built by multiplying eq. 13 – with *all* parameters fixed as from DS and TOSCA experiments– with eq. 14:

$$S(Q,t) \,= S_{loc}(Q,t) S_\alpha(Q,t) \tag{15}$$

Thereby, only two parameters were allowed to float: A and $\tau_w(Q)$. The resulting descriptions were very satisfactory, with the characteristic times displayed in Fig. 10.

Analysis of dry PDMAEMA QENS data. Here the value of σ_β was fixed to that extrapolated from DS results. The obtained fitting curves describe reasonably well the data and are displayed in Fig. 11 (dashed lines) for T=290 K. The value of $< \overline{\log(\tau)} >_Q$ for this temperature is included in Fig. 9 and is about a factor of 8 larger than that from DS.

Analysis of PDMAEMA/H_2O QENS data. Since no information about the dielectric β-relaxation is accessible in this case, we fixed the σ_β value to that obtained by DS in the PDMAEMA/THF mixture. Figure 12 shows with the dashed lines the best description of the incoherent scattering function achieved, corresponding to the average value of the characteristic time displayed in Fig. 9. This characteristic time is significantly larger than that obtained for the mixture with THF.

IV. Discussion

α-Relaxation. We find, as usually reported[26,27], a decrease of the glass transition temperature T_g of the polymer upon addition of solvents. This can be directly observed from the DSC investigation for the two mixtures (arrows in Fig. 2 and Fig. 4(a), top). The shift induced by both solvents is nearly the same, but the presence of water leads to a much broader signature

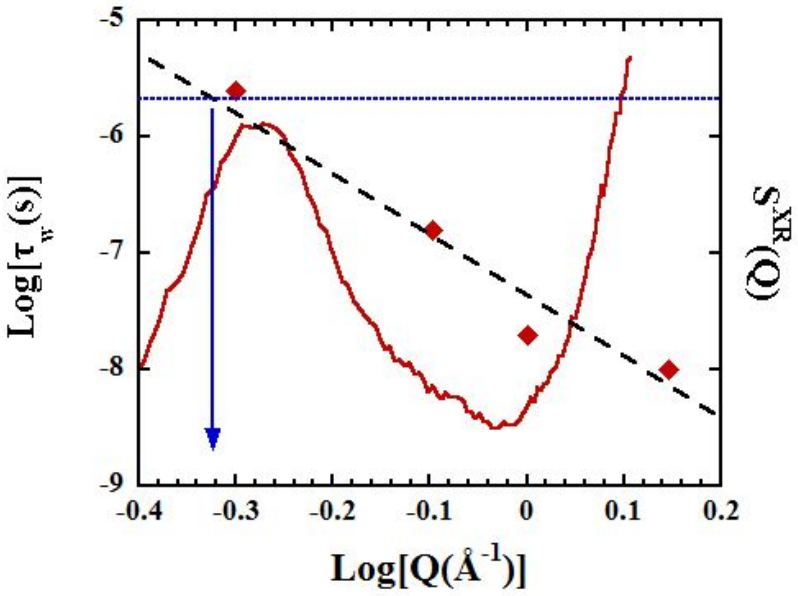

Figure 10: Wavevector dependence of the characteristic times of the stretched exponential function characterizing the intermediate scattering function of the α-relaxation in the mixture with THF at 290K. Dashed line is a power law $\tau_w \propto Q^{-2/\beta}$ corresponding to Gaussian behaviour. The horizontal dotted line indicates the value of the corresponding characteristic time τ_w deduced from the dielectric spectroscopy study and the vertical arrow marks the location of the Q-value at which this time matches the NS results. For comparison, the static structure factor measured by X-ray diffraction on this system has also been included (continuous line).

of the glass transition (Fig. 4(a), top). This effect might be a consequence of the hydrogen bonds formed in the aqueous mixture. From the FWHM of the loss peak (Fig. 5(a)), we can see that the dielectric characterization of the PDMAEMA α-relaxation in the dry state reveals a strong dynamic heterogeneity at low temperatures, approaching T_g, that becomes less relevant as the temperature increases. In the polymer mixture with THF, we observe an extra broadening at high temperature that could be associated to concentration fluctuations.

Regarding the T-dependence of the relaxation time, the polymer in the mixture with

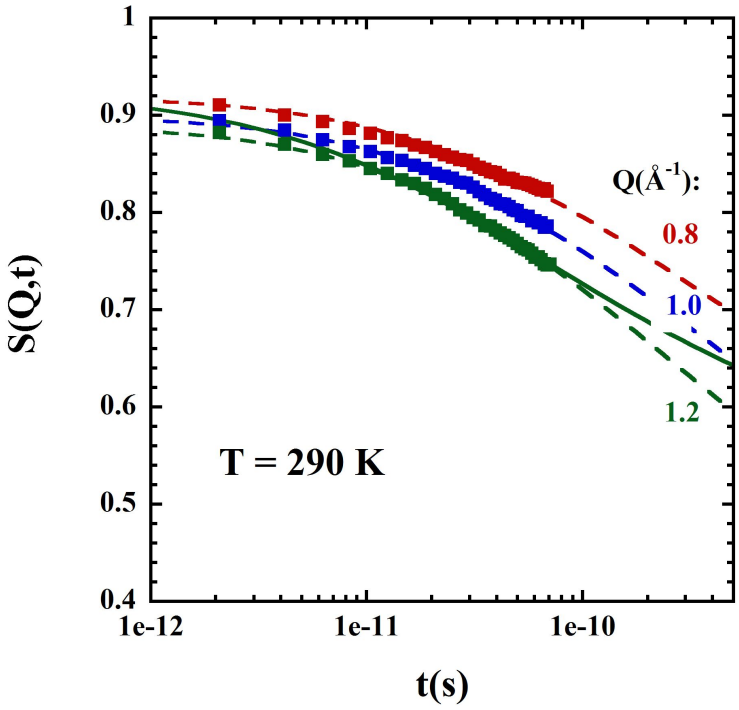

Figure 11: Intermediate scattering function of PDMAEMA hydrogens in the dry sample at T=290K and the different Q-values indicated described by eq. 13 (dashed line). Solid line is the description of the highest-Q results by assuming a fraction of slow atoms (see the text).

THF appears less 'fragile' in the Angell clasification[15] than in the dry system. As can be seen in Table 2, the parameter m drastically changes with THF addition, leading to a much less fragile behaviour. This observation is in agreement with typical plasticizing effects reported in literature (e.g. polyvinyl chloride (PVC) and PVC with dioctyl phthalate (DOP)[27], poly(vinyl methyl ether) PVME/H_2O[26]).

Now we focus on the changes induced in the glass-transition temperature of the polymer observed by DS and DSC. The shift deduced from DS analysis is 83 K, rather stronger than that obtained from DSC from the inflection point (i.e., from the maximum of the C_p^{Rev} derivative (see Fig. 4(a))). However, this apparent discrepancy between the observation by the two techniques disappears if we consider the onset temperature $T_{g,onset}^{DSC}$ (see Table 2 and

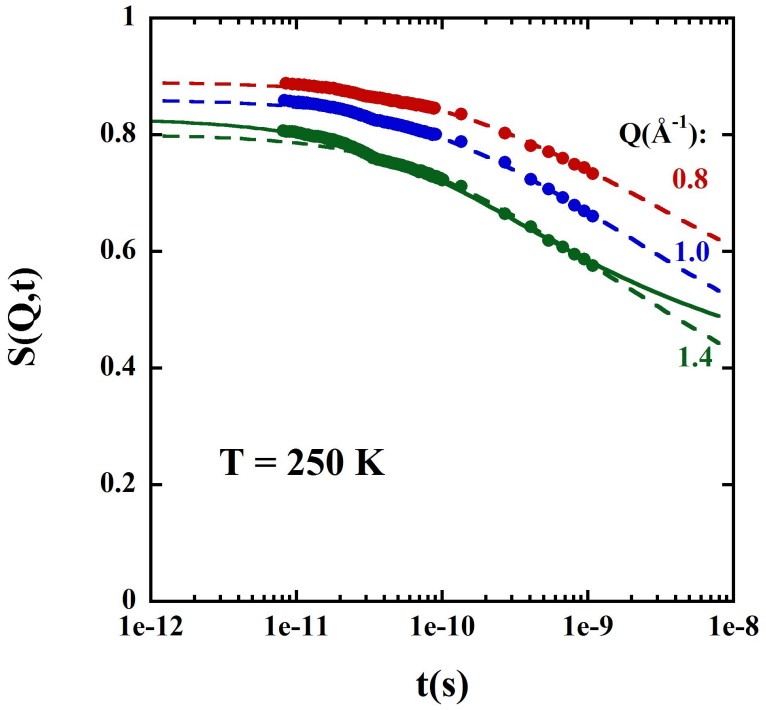

Figure 12: Intermediate scattering function of PDMAEMA hydrogens in PDMAEMA/D_2O at T=250K and the different Q-values indicated described by eq. 13 (dashed line). Solid line is the description of the highest-Q results by assuming a fraction of slow atoms (see the text).

Fig. 4(a) top). Noteworthy, the values of the glass-transition temperatures T_g^{DS} and $T_{g,onset}^{DSC}$ nearly coincide for both systems. This indicates that dielectric relaxation is very sensitive to the onset of the molecular motions involved in the glass-transition. In the particular case of PDMAEMA, this could be related with the fact that the dipole moment is mainly associated to the side group. Such feature would also explain the above observed large broadening of the dielectric relaxation close to the glass-transition ($\sim$ 4 decades in both dry and mixture). Similar behavior has been observed in other systems with bulky side groups like poly(n-alkyl methacrylates) (PnMAs)[28].

Finally, we note that the analysis of the highest temperature QENS data on the PDMAEMA/THF mixture has allowed extracting information on the contribution of the α-relaxation to the

polymer atomic motions. As expected, the characteristic times deduced for this process show a strong dispersion with Q (see Fig. 10), which can be rather well described by the power law $\tau_w \propto Q^{-2/\beta}$ corresponding to the Gaussian approximation[29–32]. In this figure we have also included the value of the characteristic time obtained from DS for the α-relaxation. This value agrees with the value expected for $\tau_w(Q)$ at $Q \sim 0.4$ Å^{-1}. It has usually been reported that such a coincidence occurs for $Q \sim 1$Å^{-1} in glass-forming polymers[33]. However, for polymers like poly(vinyl acetate) (PVAc) and poly(alkylene oxide)s (PAOs) –also with relatively bulky side groups– it has been found that the matching takes place at lower Q-values, which have been identified –within the experimental uncertainties– with the Q-value Q_{max} corresponding to the inter-chain correlations of the static structure factor S(Q)[34,35]. In Fig. 10 we have also represented the results for S(Q) as measured by X-ray diffraction on the PDMAEMA/THF sample. As can be seen in this figure, the coincidence of DS and QENS characteristic times for the α-relaxation of PDMAEMA in the mixture with THF also takes place around Q_{max}.

Methyl-Groups Dynamics. TOSCA experiments have allowed a detailed characterization of PDMAEMA methyl-group dynamics. The values of the average potential barrier and the widths of the distribution functions of the MC-MG are in the range of MC-MGs in vinylic polymers as polyisobutylene (PIB),[36–38] poly(α-methylstyrene) (PαMS),[39] and poly(methyl methacrylate) (PMMA).[39] Conversely, the average values of the barrier for the SG-MG rotations are lower than those of the MC-MG. This was also the case in PMMA (ester-methyl)[40,41] and poly(ethyl methacrylate) (PEMA).[42] The obtained results in the mixtures quantitatively confirm that plasticization does not significantly produce either a shift of the average value or an extra broadening of the distribution function of potential barriers.

Localized Side-Group Motions of PDMAEMA in the Glassy State. Dielectric spectroscopy reveals local motions under the so-called β-relaxation. A significant change of this process occurs in the presence of THF molecules ('process II'). Polymer dynamics appear faster in THF solution and the apparent activation energy is affected by the presence of THF

molecules (Table 3). Moreover, a strong reduction of the dielectric strength (Fig. 3(b)) and a narrowing of the characteristic relaxation times distribution (Fig. 5(b)) are found. These observations resemble the situation reported for PVC upon addition of DOP[27]. In that case, this was attributed, as in the case of Bisphenol-A Polycarbonate[43], to the presence of two distinct contributions (a fast and a slow component) to the dielectric β-relaxation of the neat polymer. At high temperature, the fast component would dominate the dipole reorientation, while, as the temperature decreases, the slow component would get more relevance. When comparing the results obtained for the dry polymer and in the mixture, we observe a rather good agreement at high temperature regarding both the characteristic time (points in Fig. 9) and the width of the distribution (bars in Fig. 9). On the contrary, at low T the distribution in the mixture remains about the same as at high T, while in the dry polymer a much broader distribution is found. In addition, the average time of such distribution is larger in the dry polymer than in the mixture. These results could be rationalized on the basis of the existence of two components in the dry system. At high T the fast component would dominate in both samples. At low T, the β-process in the mixture would reflect only the fast component (with similar distribution width as at high T). This suggests to identify the fast component of the β-relaxation in the dry polymer with the single process detected in the mixture. Therefore, it would be characterized by the parameters shown in Table 3 corresponding to PDMAEMA in the mixture with THF. In the dry state, the presence of a slower component would be evidenced by the broader distribution and the larger average time at low T. We may estimate the relaxation time characteristic for the slow component τ^{slow} in the following way. First, a value can be estimated from the lowest temperature results (T=140 K). Assuming that the distribution width of the fast relaxation time of the dry polymer is similar to the one of the polymer in the mixture (as at high T), the non-overlapping zone of the bars at such low T (see Fig. 9) could be attributed to the distribution of the characteristic time of the slow component. Thus, such distribution spans over the range $-0.2 < \log(\tau(s)) < -2.4$. The characteristic time τ^{slow} could be determined from the center of this interval, namely

$\log[\tau^{slow}(s)](T = 140\ K) = -1.3$. Now, assuming an Arrhenius law with the same pre-factor as that for the fast component, the dotted line in Fig. 9 has been obtained for τ^{slow}. The corresponding activation energy would be ∼31 kJ/mol.

Dielectric spectroscopy provides an insight into the molecular motions through the dipole-dipole correlation function; direct information at atomic scale is revealed by QENS. The QENS results have allowed selectively following the hydrogen dynamics of the polymer component in the systems. For PDMAEMA in the mixture with THF at 250 K, they have revealed side-group localized motions with similar characteristics of the dielectric β-process. This agreement allows to assume that in this case QENS is sensitive to the microscopic motions responsible for the β-relaxation detected by DS. These data can be well described by assuming for the localized motions of side groups confined rotations on discs of 3 Å radius for methylene hydrogens and 1.65 Å radius for methyl-group hydrogens. Thus, we have been able to estimate the spatial extent of the localized motions involved in the β-relaxation of the polymer in the mixture with THF. We note that this description could also be extensible to higher temperatures, if the α-process contribution is considered.

We now discuss the QENS results on the dry sample. We have deduced a characteristic time scale for H-motions about 8-fold longer than that observed in the mixture with THF (see Fig. 9). Interestingly, the QENS time found for dry PDMAEMA is close to that estimated from DS for the slow component of the β-relaxation. This observation suggests the presence of a slow proton population in the dry polymer. Such a fraction of slowly moving atoms was not considered in the previous analysis. Therefore, we have reconsidered the model used to describe the QENS data on the dry polymer. In this high temperature range, DS results show coincident time scales for both, dry polymer and in the mixture. This is indicative of the existence of a common molecular motion, that can be identified as that detected and characterized by QENS in the mixture. Thus, for describing the intermediate scattering function of hydrogens in the dry sample, we assume a combination of a fraction f of protons undergoing the molecular motion in common and the rest *(1-f)* being much slower and giving

an effectively elastic signal in the accessible dynamic window:

$$S^{dryPDMAEMA}(Q,t) = fS^{PDMAEMA/THF}(Q,t) + (1-f)A \tag{16}$$

Here $S^{PDMAEMA/THF}(Q,t)$ is given by Eq. 13 and A is the common pre-factor accounting for faster processes. This model describes well the data of the dry polymer for all Q-values and temperatures investigated (250, 270 and 290 K) with a value of $f = 0.65$ (see as an example the solid line in Fig. 11).

The analysis of the QENS data on the aqueous mixture lead to a similar situation: the characteristic time found is again larger than that obtained for the THF mixture. Also in this case we may assume a slower component in the intermediate scattering function. Reanalyzing the data with Eq. 16 we also obtain a nice description of the experimental QENS data (see Fig. 12) with a value of $f = 0.75$.

After this synergetic approach combining the results from both DS and QENS techniques we can propose the following scenario: in the dry polymer, two (fast and slow) local molecular motions coexist, both controlling the dielectric relaxation –dipole reorientations– at low temperature. Addition of solvent molecules seems not to affect significantly the fast motion, but reduces the population involved in the slow process. This reduction is nearly complete in the THF mixture. However, water molecules produce only a partial reduction. The observed reduction of the slow motions in the mixtures could be attributed to the release of the steric hindrance and/or to a weakening of some interactions between side-groups. In the case of the THF mixture, there is a one-to-one ratio between solvent molecules and monomeric units, which would be sufficient for a nearly complete effect. In the water mixture, there is a 4:1 ratio between water molecules and monomers. However, it is well known the tendency of water to form clusters by H-bond interactions. Formation of clusters of water molecules of different sizes could give rise to a non-homogeneous distribution of water molecules at the monomeric level. In agreement with this idea, we recall the extremely broad glass-transition

feature observed by DSC on this sample (see Fig. 4(a), top). In this framework, the remaining slow fraction of side-groups hydrogens in the aqueous mixture would be due to the presence of some regions with a low hydration level. Given the pronounced effect observed on the DSC trace, we may suggest a typical size in the nano-meter range for these regions.

Conclusions

We have addressed the question how the presence of plasticizers –THF and H_2O– affects PDMAEMA dynamics at different levels by combining DSC, dielectric spectroscopy and neutron scattering techniques. Unfortunately, DS fails in giving information about the polymer component in the aqueous mixture due to the overwhelming signal of water. Despite this fact, interesting conclusions can be drawn:

(i) The α-relaxation of the polymer is drastically affected. DSC shows strong shifts of the glass-transition temperature, with similar values for both solvents but a much more pronounced broadening for the aqueous mixture. In addition, DS reveals effects of compositional heterogeneities at high temperatures and a strong reduction of the fragility upon addition of THF.

(ii) On the other extreme, methyl-group dynamics are unaffected by solvents.

(iii) The synergetic analysis of DS and QENS results on dry PDMAEMA and its mixture with THF suggests two kinds of side-group molecular motions –a slow and a fast one– contributing to the β-process in the dry state. Based on the spatial information provided by QENS, a model for the geometry of the motions involved in the fast process has been proposed. Upon addition of solvent, this process would remain essentially unaltered, while the population involved in the slower one would be reduced. This reduction would be complete, within the experimental uncertainties, in the THF mixtures, but only partial in the aqueous systems.

(iv) Both, the more pronounced broadening of the glass-transition region and the weaker

influence on the local side-group motions of the polymer produced by the presence of water, with respect to THF, could be attributed to the possible existence of clusters of water molecules heterogeneously distributed in the polymeric matrix. This would be the main difference introduced by the capability of H-bond formation of water molecules in contrast to the case of THF molecules.

Acknowledgements

Financial support from the Projects MAT2012-31088 (Spanish-MINECO and EU) and IT-654-13 (Basque Government) is acknowledged. This work is based on experiments performed at FOCUS (SINQ, Paul Scherrer Institute, Villigen, Switzerland), and at TOFTOF and SPHERES (Heinz Maier-Leibnitz Zentrum (MLZ), Garching, Germany), and has been supported by the European Commission under the 7th Framework Programme through the 'Research Infrastructures' action of the 'Capacities' Programme, NMI3-II Grant Number 283883.

References

(1) Kenawy, E.-R.; Worley, S.; Broughton, R. *Biomacromolecules* **2007**, *8*, 1359–1384.

(2) Asadinezhad, A.; Novák, I.; Lehocký, M.; Sedlařík, V.; Vesel, A.; Junkar, I.; Sáha, P.; Chodák, I. *Colloids and Surfaces B: Biointerfaces* **2010**, *77*, 246–256.

(3) Wang, H.; Wang, L.; Zhang, P.; Yuan, L.; Yu, Q.; Chen, H. *Colloids and Surfaces B: Biointerfaces* **2011**, *83*, 355–359.

(4) Lin, S.; Du, F.; Wang, Y.; Ji, S.; Liang, D.; Yu, L.; Li, Z. *Biomacromolecules* **2007**, *9*, 109–115.

(5) Wagner, E.; Kloeckner, J. *Polymer Therapeutics I* **2006**, 135–173.

(6) Richter, D.; Monkenbusch, M.; Arbe, A.; Colmenero, J. *Neutron Spin Echo in Polymer Systems* **2005**, 1–221.

(7) Bée, M. *Quasielastic Neutron Scattering:*; Adam Hilger, 1988.

(8) Lovesey, S. W. *Theory of Neutron Scattering from Condensed Matter*; Clarendon Press, Oxford, 1984.

(9) Squires, G. L. *Introduction to thermal neutron scattering*; Cambridge university press, 1988.

(10) Kremer, F., Schönhals, A., Eds. *Broadband Dielectric Spectroscopy*, 2003rd ed.; Springer, 2002.

(11) Wübbenhorst, M.; van Turnhout, J. *Dielectric Newsletter* **2000**, 1–3.

(12) Vogel, H. *Phys. Z* **1921**, *22*, 645–646.

(13) Fulcher, G. S. *Journal of the American Ceramic Society* **1925**, *8*, 339–355.

(14) Tammann, G.; Hesse, W. *Zeitschrift für anorganische und allgemeine Chemie* **1926**, *156*, 245–257.

(15) Angell, C. A. *Science* **1995**, *267*, 1924–1935.

(16) Schwartz, G. A.; Colmenero, J.; Alegría, Á. *Macromolecules* **2007**, *40*, 3246–3255.

(17) Goracci, G.; Arbe, A.; Alegría, W., A Lohstroh; Su, Y.; Colmenero, J. *J. Chem. Phys.* submitted.

(18) Blochowicz, T.; Lusceac, S.; Gutfreund, P.; Schramm, S.; Stuhn, B. *The Journal of Physical Chemistry B* **2011**, *115*, 1623–1637.

(19) Bock, D.; Kahlau, R.; Pötzschner, B.; Körber, T.; Wagner, E.; Rössler, E. *J. Chem. Phys.* **2014**, *140*, 094505.

(20) Kahlau, R.; Bock, D.; Schmidtke, B.; Rössler, E. *J. Chem. Phys.* **2014**, *140*, 044509.

(21) This equation resulted from the CC fit of the loss-curves generated with a superposition of Debye relaxations according to eq. 8 for various σ-values in the range from 0.1 to 0.5.

(22) Peterlin-Neumaier, T.; Springer, T. *J. of Polym. Sci.: Polym. Phys. Ed.* **1976**, *14*, 1351.

(23) Colmenero, J.; Moreno, A. J.; Alegría, A. *Progress in polymer science* **2005**, *30*, 1147–1184.

(24) Chahid, A.; Alegria, A.; Colmenero, J. *Macromolecules* **1994**, *27*, 3282–3288.

(25) Colmenero, J.; Mukhopadhyay, R.; Alegria, A.; Frick, B. *Physical review letters* **1998**, *80*, 2350.

(26) Capponi, S.; Arbe, A.; Cerveny, S.; Busselez, R.; Frick, B.; Embs, J.; Colmenero, J. *The Journal of chemical physics* **2011**, *134*, 204906.

(27) Zorn, R.; Monkenbusch, M.; Richter, D.; Alegría, A.; Colmenero, J.; Farago, B. *The Journal of chemical physics* **2006**, *125*, 154904.

(28) Arbe, A.; Genix, A.-C.; Arrese-Igor, S.; Colmenero, J.; Richter, D. *Macromolecules* **2010**, *43*, 3107–3119.

(29) Arbe, A.; Colmenero, J.; Alvarez, F.; Monkenbusch, M.; Richter, D.; Farago, B.; Frick, B. *Physical review letters* **2002**, *89*, 245701.

(30) Farago, B.; Arbe, A.; Colmenero, J.; Faust, R.; Buchenau, U.; Richter, D. *Physical Review E* **2002**, *65*, 051803.

(31) Colmenero, J.; Alegria, A.; Arbe, A.; Frick, B. *Physical review letters* **1992**, *69*, 478.

(32) Colmenero, J.; Arbe, A.; Alegria, A.; Monkenbusch, M.; Richter, D. *Journal of Physics: Condensed Matter* **1999**, *11*, A363.

(33) Colmenero, J.; Arbe, A.; Alegría, A. *J. Non-Cryst. Solids* **1994**, *172-174*, 126–137.

(34) Tyagi, M.; Arbe, A.; Alvarez, F.; Colmenero, J.; Gonzalez, M. A. *J. Chem. Phys.* **2008**, *129*, 224903.

(35) Gerstl, C.; Schneider, G. J.; Fuxman, A.; Zamponi, M.; Frick, B.; Seydel, T.; Koza, M.; Genix, A.-C.; Allgaier, J.; Richter, D.; Colmenero, J.; Arbe, A. *Macromolecules* **2012**, *45*, 4394–4405.

(36) Annis, B.; Lohse, D.; Trouw, F. *The Journal of chemical physics* **1999**, *111*, 1699–1704.

(37) Adams, M. A.; Gabrys, B. J.; Zajac, W. M.; Peiffer, D. G. *Macromolecules* **2005**, *38*, 160–166.

(38) Frick, B.; Richter, D.; Trevino, S. *Physica A: Statistical Mechanics and its Applications* **1993**, *201*, 88–94.

(39) Allen, G.; Wright, C.; Higgins, J. *Polymer* **1974**, *15*, 319–322.

(40) Moreno, A.; Alegria, A.; Colmenero, J.; Frick, B. *Physical Review B* **1999**, *59*, 5983.

(41) Moreno, A.; Alegría, A.; Colmenero, J.; Frick, B. *Macromolecules* **2001**, *34*, 4886–4896.

(42) Genix, A.-C.; Arbe, A.; Colmenero, J.; Wuttke, J.; Richter, D. *Macromolecules* **2012**, *45*, 2522–2536.

(43) Alegría, A.; Mitxelena, O.; Colmenero, J. *Macromolecules* **2006**, *39*, 2691–2699.

FOR TABLE OF CONTENTS USE ONLY

'Influence of solvent on poly(2-(dimethylamino)ethyl methacrylate) dynamics in polymer-concentrated mixtures: a combined neutron scattering, dielectric spectroscopy and calorimetric study'

G. Goracci, A. Arbe, A. Alegría, V. García Sakai, S. Rudić, G.J. Schneider, W. Lohstroh, F. Juranyi and J. Colmenero